Available online at www.sciencedirect.com

ScienceDirect

Focus Article, *Mendeleev Commun.*, 2022, **32**, 287–297

Mendeleev Communications

Recent progress in lithium-ion and lithium metal batteries

Daria Yu. Voropaeva,[a] Ekaterina Yu. Safronova,[a] Svetlana A. Novikova[a] and Andrey B. Yaroslavtsev*[a,b]

[a] *N. S. Kurnakov Institute of General and Inorganic Chemistry, Russian Academy of Sciences, 119991 Moscow, Russian Federation. E-mail: yaroslav@igic.ras.ru*
[b] *HSE University (National Research University Higher School of Economics), 119048 Moscow, Russian Federation*

DOI: 10.1016/j.mencom.2022.05.001

Moving towards carbon-free energy and global commercialization of electric vehicles stimulated extensive development in the field of lithium-ion batteries (LIBs), and to date, many scientific and technological advances have been achieved. The number of research works devoted to developing high-capacity and stable materials for lithium-ion and lithium metal batteries (LMBs) is constantly rising. This review covers the main progress in the development of LIBs and LMBs based on research works published in 2021. One of the main goals in the recent publications is to solve the problem of instability of layered nickel-rich lithium–nickel–cobalt–manganese oxides (Ni-rich NMC) cathodes, as well as silicon anodes. Improving the stability of NMC cathodes can be achieved by doping them with cations as well as by coating the oxides' surfaces with protective layers (organic polymers and inorganic materials). The most effective strategies for dampening volumetric changes in silicon anodes include using porous silicon structures, obtaining composites with carbon, coating silicon-containing particles with inorganic or polymeric materials, and replacing standard binder materials. Much work has been devoted to suppressing dendrite formation in LMBs by forming stable coating layers on the surface of lithium metal, preparing composite anodes and alloys, and changing the composition of electrolytes. At the same time, in the field of electrolyte development, many research works have been devoted to the search for new hybrid polymer electrolytes containing lithium-conducting inorganic materials.

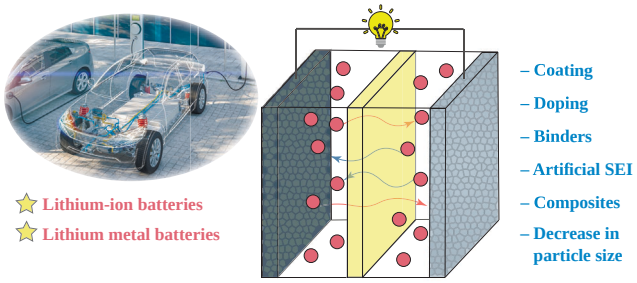

Keywords: lithium-ion battery, lithium metal battery, cathode materials, NMC, anode materials, silicon anode, hybrid polymer electrolyte.

1. Introduction

Switching to the carbon-free energy has stimulated the recent development of scientific and technological progress in the field of electrochemical energy storage.[1–3] Electric vehicles can significantly reduce greenhouse gas emissions and air pollution compared to internal combustion engine vehicles and thus are a key strategy to reduce emissions. High demand for lithium-ion batteries (LIBs) used as an alternative energy source in electric and hybrid vehicles, as well as stationary energy storage at renewable energy power plants, is inevitably growing.[4–7] The main trends in LIBs improvement are stimulated by the need to increase the range of electric vehicles, improve their safety, lifetime and reduce their cost. The U.S. Advanced Battery Consortium (USABC) has issued end-of-life battery specifications for electric vehicles, which are defined by a reduction in battery capacity to 80% of the initial level (Table 1).[8,9]

Table 1 Key end-of-life battery performance targets for electric vehicles to be achieved by 2025, according to USABC.

Cathode capacity (C/3 charge and discharge)/mA h g^{-1}	Anode capacity (C/3 charge and discharge)/mA h g^{-1}	Operating voltage *vs.* Li/Li^+ /V	Time of charging up to 80% of full capacity/min	Cycle life	Calendar life/ years	Specific energy/ W h kg^{-1}	Energy density/ W h dm^{-3}
>250	>2000	1.0–4.3	15	>1000	>15	350	750

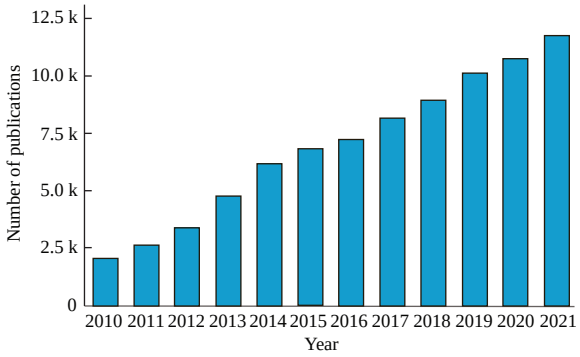

Figure 1 Analysis of publication activity on the topic 'lithium-ion batteries' according to the Scopus database.

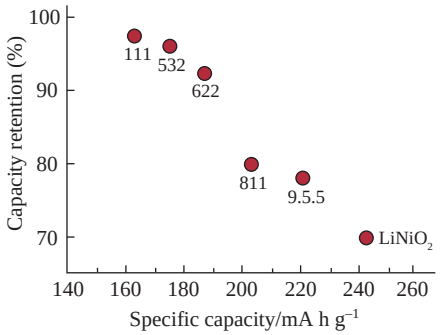

Figure 2 Dependence of capacity retention on specific capacity after 100 cycles of different NMC cathodes. The numbers indicate the ratio of metals in the NMC cathode. Plotted from the data.[14]

To achieve these goals, new materials with higher energy density or modification of existing materials, improved battery designs, and new electrochemical energy systems such as lithium metal, lithium-air, sodium-ion, metal–sulfur batteries, *etc*., are developed. In this regard, a steady increase in the number of research works devoted to developing LIBs can be observed (Figure 1). The purpose of this review is to illuminate the main progress in the improvement of LIBs and lithium metal batteries (LMBs) based on the analysis of works published in 2021.

2. Lithium-ion batteries

2.1. Cathode materials

The cathode is one of the main components of the LIBs, which determines its capacity. Recent developments in cathode chemistry focus on increasing energy density, cyclability and safety, and reducing the cost of materials. The most commonly used cathodes for electric vehicle batteries are mixed nickel–manganese–cobalt–lithium oxides $LiNi_xMn_yCo_{1-x-y}O_2$ (NMC523, NMC622, NMC811, *etc*., where transition metal symbols are limited to the first letter and numbers indicate transition metal ratios), nickel–cobalt–aluminum–lithium oxide ($LiNi_xCo_yAl_{1-x-y}O_2$, NCA), and lithium–iron phosphate ($LiFePO_4$, LFP).[10]

2.1.1. Layered oxides

In NMC cathode materials, several transition metals have an effect on material characteristics: Ni provides high capacity, Mn stabilizes the structure, and Co reduces the concentration of defects in the exchange of Li^+ and M^{2+} cations positions.[11,12] Such materials have a layered structure, with lithium intercalation/deintercalation processes occurring in the space between layers by solid-solution reaction, promoting continuous crystal structure change.[13] Increasing the nickel content improves the capacity and energy density of the battery and reduces the cost. However, an increase of the nickel concentration in NMC cathodes significantly reduces the cyclability due to substantial degradation of the material (Figure 2).[14]

The main disadvantages of NMC cathodes include the formation of microcracks and the possibility of oxygen release during cycling, which eventually leads to low stability, as well as makes the battery operation unsafe.[15,16] Moreover, with high lithium intercalation/deintercalation rates, the Li^+ concentration gradient inside the particle can increase, causing internal stresses and cracks.[13]

Recent research work[17] showed that the oxygen release during the operation of NMC cathodes is caused by the formation of holes in the valence band during the charging process, which leads to oxygen activation. Released oxygen can then oxidize the electrolyte and reduce the number of transition metals on the particle surface, followed by irreversible phase transformations from the layered structure of NMC to spinel and/or rock-salt structure[16] which on the other hand leads to the formation of cracks and an overall decrease in battery capacity.[18]

Two main approaches are considered to improve the stability of NMC cathodes: doping with other cations and protective coating. Usually, dopant ions with small ionic radius, such as Al^{3+}, Mg^{2+}, hold Li^+ positions and stabilize the interlayer distance during intercalation/deintercalation.[19–21] Doping with polyvalent cations with larger ionic radius (Nb, Mo, Zr, W) also can stabilizes the NMC structure. For example, it was shown, that doping $LiNi_{0.89}Co_{0.055}Mn_{0.055}$ cathode with Zr^{4+} or Mo^{6+} ions can lead to the improvement of the stability and electrochemical characteristics, as well as to the reduction oxygen evolution.[22] Doping $LiNi_{0.6}Co_{0.05}Mn_{0.3}O_2$ cathode with 2 mol% titanium improves lithium diffusion and suppresses undesirable phase transition.[23] Doping NMC622 with aluminum

Daria Yu. Voropaeva is a post-graduate student and Junior Researcher at the Laboratory of Ionics of Functional Materials, Kurnakov Institute of General and Inorganic Chemistry RAS. Her current research interests are devoted to investigation of single-ion conducting polymer electrolytes for application in metal-ion batteries.

Ekaterina Yu. Safronova is a Senior Researcher at the Laboratory of Ionics of Functional Materials, Kurnakov Institute of General and Inorganic Chemistry RAS. Her current research interests include investigation and design of ion-exchange membranes, including hybrid nanomaterials for fuel cells, potentiometric sensors and water treatment. She is a co-author of over 88 articles and 5 patents.

Svetlana A. Novikova is a Senior Researcher at the Laboratory of Ionics of Functional Materials, Kurnakov Institute of General and Inorganic Chemistry RAS. Her research focuses on the development of cathode materials and polymer electrolytes for metal-ion batteries. She is a co-author of over 58 publication and 2 patents.

Andrey B. Yaroslavtsev, Corresponding Member of the Russian Academy of Sciences, the head of the Laboratory of Functional Materials Ionics, Kurnakov Institute of General and Inorganic Chemistry, Russian Academy of Sciences. His fields of scientific activity are materials science, membrane science and technology, solid-state chemistry and solid-state ionics. He is an author of about 500 peer-reviewed publications. The main areas of his research activities are related to the investigation of ionic mobility in solids, including solid electrolytes and membrane materials.

Table 2 Initial capacity and cyclic stability of modified NMC cathodes.

Material	C-rate	Initial capacity/mA h g^{-1}	Capacity drop per cycle (%)	Cycle numbers	Ref.
$LiNi_{0.6}Co_{0.17}Mn_{0.2}Al_{0.03}O_2$	0.3C	143	0.086	200	19
Ti^{4+} doping of $LiNi_{0.6}Co_{0.05}Mn_{0.35}O_2$	1C	187	0.041	500	23
$LiNi_{0.5}Mn_{1.4}Sr_{0.1}O_4$	1C	134	0.027	500	28
Al^{3+}, Zr^{4+} doping and Li_2ZrO_3 coating on NMC622	1C	167	0.199	100	24
Ca^{2+} doping and phosphate coating on $LiNi_{0.91}Co_{0.06}Mn_{0.03}O_2$	0.5C	193	0.276	80	47
$TiNb_2O_7$ coating on $LiNi_{0.88}Co_{0.06}Mn_{0.06}O_2$	1C	~180	0.064	200	31
TiN coating on NMC811	0.4C	199	0.119	200	33
TiN and polypyrrole coatings on NMC811	1C	~180	0.037	800	34
TiO_x coating on NMC622	1C	~170	~0.065	100	32
Nb doping and $LiBO_2$ coating on NMC532	0.5C	141	0.182	50	36
Zr^{4+} doping and $LiBO_2$ coating on $LiNi_{0.82}Co_{0.13}Mn_{0.05}O_2$	1C	180	0.037	250	48
$VOPO_4$ coating on $Li_{1.2}Mn_{0.54}Ni_{0.13}Co_{0.13}O_2$	1C	223	0.080	100	35
$Li_xZr_yPO_z$ coating on NMC811	1C	190	0.208	100	37
$Li_2AlZr(PO_4)_3$ coating on $LiNi_{0.92}Co_{0.05}Mn_{0.03}O_2$	0.5C	231	0.094	400	38
$Li_7La_3Zr_2O_{12}$ coating on $Li_{1.2}Ni_{0.13}Co_{0.13}Mn_{0.54}O_2$	0.5C	~230	~0.120	400	43
$Li_n(TM)_mPO_4$ coating on NMC811	1C	~205	0.065	300	41
Li_3PO_4 coating on $Li_{0.98}Mg_{0.01}Ni_{0.83}Co_{0.11}Mn_{0.06}O_2$	2C	175	0.037	500	20
LiPON coating on NMC811/graphite	0.5C	175	0.069	288	45
α-$LiAlO_2$ coating on $LiNi_{0.8}Co_{0.15}Al_{0.05}O_2$	5C	178	0.150	200	44
Ta_2O_5 coating on $LiNi_{0.8}Co_{0.15}Al_{0.05}O_2$	1C	193	0.028	200	30
Al_2O_3 and PEDOT coatings on $LiNi_{0.8}Co_{0.15}Al_{0.05}O_2$	2C	171	0.024	500	29

and zirconium provides 92.1% capacity retention compared to 76.3% for undoped NMC622 after 100 cycles at 1C rate.[24] Additionally, $LiNi_{0.8}Fe_{0.1}Mn_{0.1}O_2$ material provided a capacity of 202.6 mA h g^{-1} at 0.1C rate and 81.1% capacity retention after 150 cycles at 10C.[25] Moreover, $LiNi_{0.94}Co_{0.04}Zn_{0.02}O_{1.99}$ cathode retains 74% of its initial capacity after 500 cycles in a battery with a graphite anode.[26] Doping lithium–manganese–nickel oxide cathodes with potassium or strontium improves its cyclability. While potassium doping and carbon coating provide only a 1.5% capacity loss after 200 cycles,[27] introduction of the strontium to the material $LiNi_{0.5}Mn_{1.5-x}Sr_xO_4$ (x = 0, 0.05, 0.1, 0.15 and 0.2) shows 87% capacity retention after 500 cycles at 1C rate.[28]

The two main factors promoting the surface degradation of NMC cathodes are changes in the surface structure and reactions with the electrolyte. To prevent side reactions between the cathode and the organic electrolyte, the NMC surface can be modified with various materials, including metal oxides Al_2O_3,[29] Ta_2O_5,[30] $TiNb_2O_7$,[31] TiO_x[32]), nitrides (TiN[33,34]), phosphates (Zr_xPO_y, $VOPO_4$),[35] and a wide range of lithium-ion conductors [$LiBO_2$,[36] $Li_xZr_yPO_z$,[37] Li_3PO_4,[20] $LiBO_2$,[36] $Li_2AlZr(PO_4)_3$,[38] $LiNbO_3$,[39] $Li_{1.4}Y_{0.4}Ti_{1.6}(PO_4)_3$,[40] $Li_nM_mPO_4$ (M = Ni, Co, Mn),[41] $LiAlSiO_4$,[42] $Li_7La_3Zr_2O_{12}$,[43] α-$LiAlO_2$,[44] $Li_xPO_yN_z$ (LiPON),[45] *etc*.]. Thus, coating a $LiNi_{0.88}Co_{0.06}Mn_{0.06}O_2$ cathode with a thin layer of $TiNb_2O_7$ suppresses side reactions and provides 87.2% capacity retention after 200 cycles at 1C rate compared to the 59.8% for the native material.[31] Li-conductive coatings, in addition to their protective functions, can also increase the diffusion coefficient of lithium ions in cathode materials.[46] Thus, $Li_{1.4}Y_{0.4}Ti_{1.6}(PO_4)_3$ deposition facilitates lithium transfer and increases the cycling stability of $LiNi_{0.88}Co_{0.09}Mn_{0.03}O_2$ cathode, which results in 85% capacity retention after 1000 cycles at 0.5C.[40]

Simultaneous doping and protective coating of NMC cathodes lead to a significant improvement of the material characteristics. Thus, $LiNi_{0.91}Co_{0.06}Mn_{0.03}O_2$ cathode doping with calcium and simultaneous phosphate coating on the particle surface increases the cycling stability and provides a capacity of 210.2 mA h g^{-1} at 0.1C.[47] Coating $LiNi_{0.8}Co_{0.15}Al_{0.05}O_2$ cathode with tantalum oxide followed by doping with Ta^{5+} ions results in 94.5% capacity retention after 200 cycles at 1C, while the native material shows only 61.0% capacity retention.[31] $LiNi_{0.82}Co_{0.13}Mn_{0.05}O_2$ doping with Zr^{4+} ions followed by $LiBO_2$ coating increases the capacity to 200.8 mA h g^{-1} at 0.1C, leading to a decrease of the capacity less than 10% after 250 cycles at 1C.[48]

NMC cathodes have relatively high conductivity; therefore, the surface of the cathode is usually not coated with carbon materials.[49] However, coating with conductive polymers such as poly(3,4-ethylenedioxythiophene),[29] poly(pyrrole-*co*-citral nitrile),[50] polypyrrole[34] can increase the capacity and improve cycling stability. Thus, $LiNi_{0.8}Co_{0.15}Al_{0.05}O_2$ coating with poly(3,4-ethylenedioxythiophene) and Al_2O_3, increases cathode material capacity from 194 to 209 mA h g^{-1}.[29] The main results of improving stability of NMC cathodes are summarized in Table 2.

Thus, the doping of layered oxides or applying protective organic or inorganic coatings allow one to improve their cyclic stability.

2.1.2. LFP

The $LiFePO_4$ (LFP) material with an olivine structure has several advantages: high safety, cycling stability, being environmentally friendly, and low cost. However, the capacity is lower in comparison to NMC cathodes. In 2021, the growth in demand for LFP batteries was observed,[51] which was caused by the new battery pack designs that have increased the energy density of LFP batteries to that of the NMC batteries (about 140 W h kg^{-1}), where CATL's 'cell-to-pack' concept and BYD's blade battery system were the first examples implementing the new design.

The disadvantages of LFP cathodes are determined by their low electronic and ionic conductivity.[52] Reduction of the particle size and coating the LFP surface with carbon materials are strategies mainly used to improve the electrochemical performance of the cathode.[53] Attention of researchers is also paid to the doping of LFP with ions of other metals, including the study of the reasons for the acceleration of lithium diffusion in such systems.[54] The goal of the first strategy is to reduce the length of the diffusion path of lithium ions in nanoparticles, as the charge time to a specific capacity is inversely proportional to the square of the particle size according to Fick's law of

diffusion.[55] Thus, decreasing the LFP particle size leads to an increase of the cathode capacity at high C-rates, *e.g.*, reduction of the cathode particle size to 150–350 nm, results in a 2.5% capacity decrease after 100 cycles at 0.5C, while a cathode with the particle size of 300–500 nm has a 22.3% capacity drop.[56] Considering that lithium transport in LFP occurs through one-dimensional channels, the formation of the particles with anisotropy of a specific orientation also proves to be effective.[57]

Carbon coating is usually performed by carbonization of the carbon-containing precursor at high temperatures. The carbon layer envelops the LFP, forming a 'core–shell' structure.[58] Introduction of extended carbon nanotubes or graphene particles, including those doped with nitrogen, into the composition of conductive coatings offers additional advantages;[59,60] P,N-doped carbon deposition on LFP particles can provide a relatively high discharge capacity of 150.2 mA h g^{-1} at 1C and only 0.016% capacity decrease per cycle for 300 cycles at 2C.[58] Application of the carbon coating ensures rapid supply (withdrawal) of lithium ions from each particle along with the interfaces;[61] therefore, LFP cathodes with high capacity are currently created only with a conductive coating layer.[62–64] Additionally, conductive polymers can be used instead of carbon coating.[65] To date, a possibility of a binder replacement to create LFP cathodes is being investigated by several research groups.[66]

2.2. Anode materials

Anode materials can be divided into two types based on the electrochemical reaction mechanism.[55] The first one is intercalation-type anode materials in which, similarly to the cathodes described above, lithium intercalation/deintercalation processes take place (carbon materials, materials based on titanium oxide compounds, *etc.*), sometimes a class of metals and alloys (such as silicon, germanium, *etc.*) can be discriminated.[67] However, it is difficult to find a fundamental difference from carbon. The second type includes materials in which the charge and discharge processes occur through a chain of successive transformations. Some of the processes may be irreversible (conversion-type anode materials, including transition metal oxides, sulfides, selenides, nitrides, phosphides, *etc.*), *e.g.*, tin oxide undergoes a chain of transformations $SnO_2 \rightarrow Sn + 2Li_2O \rightarrow Li_xSn + Li_2O$, which reduce specific capacity of the anode material but often provides more reliable cycling.[55]

Certain drawbacks arise for the wide application of some materials, *e.g.*, anodes made of tin, germanium, and silicon quickly degrade due to volume expansion (250–300%) during lithium intercalation.[67] Lithium titanate is characterized by low conductivity and reduced capacity when cycling at high C-rates, which, similar to cathode materials, can be improved by carbon coatings.[68–70]

The requirements for anode materials are typically not strict, as their capacity is usually significantly higher than that of cathode materials. To meet the lifetime requirement (15 years), the prospective anode material must retain at least 70% of its initial capacity after 5000 charge–discharge cycles and be safe at temperatures from –40 to +80 °C.[71] In the commercial sector, the most used anode materials are graphite and graphite–silicon composites, and recently many efforts were put into improving the performance of these materials.

2.2.1. Carbon-based materials

The properties of carbon materials largely depend on the structure, surface defects, and presence of the functional groups.[67] Graphite is the most used anode material in commercial LIBs due to its high electrical conductivity, low operating potential, and low cost. Moreover, layered graphite structure ensures stable charge/discharge processes and exploitation safety. However, limited LiC_6 composition of lithium intercalation results in a relatively low theoretical capacity of 372 mA h g^{-1}, whereas typically, its capacity is around 330 mA h g^{-1} even at low current densities.[71,72] It was shown that laser-induced structuring of graphite anodes can increase capacity by 35% at 6–8C discharge rates, improves fast charging capability, and increases cycling stability.[73] The use of N-doped carbon nanofibers derived from cellulose and chitosan allowed to achieve a capacity of 399 mA h g^{-1} at the current density of 0.03 A g^{-1}, as well as 0.21 A g^{-1} at 1 A g^{-1}.[74] Moreover, several works provided evidence of obtaining such materials with a capacity of more than 1100 mA h g^{-1}.[71,75,76] However, previously reported data on carbon materials showing capacity significantly higher than the theoretical one has not been confirmed; therefore, additional confirmation is required.

2.2.2. Silicon-based anode materials

Materials based on silicon and silicon oxides (SiO_x) are among the most promising anode materials for LIBs due to the high theoretical capacity, availability of silicon, and low operating potential,[77–79] that is why a lot of works in the field of anode materials published in 2021 were devoted to silicon-based materials. Silicon has a theoretical capacity of 3570 mA h g^{-1} (for Li_5Si_4), almost 10 times higher than that of graphite, while the theoretical capacities of SiO_2 and SiO are 1965 and 2680 mA h g^{-1}, respectively.[80,81] Despite extensive research being done on silicon anodes, only small amounts of silicon materials (typically <10 wt%) are mixed with graphite anodes to increase the capacity of commercial batteries. This can be explained by the fact that silicon-based anodes undergo significant volumetric expansion and contraction (~300%) during cycling, resulting in mechanical failure of the anode particles and loss of electrical contact. In addition, the formation of a large amount of solid products of electrolyte reduction on their surface (solid electrolyte interface, SEI) leads to low Coulomb efficiency and poor battery life.[15,82] Moreover, low values of electronic conductivity (10^{-5}–10^{-3} S cm^{-1}) and Li^+ diffusion coefficient (10^{-14}–10^{-13} cm^2 s^{-1}) are noted for silicon anodes.[83] Effective strategies to overcome these problems, including formation of porous silicon structures, obtaining composites with carbon, and coating silicon anodes with inorganic or polymer materials, are the most common.

Graphite,[81,84] carbon nanotubes (CNTs),[85–87] graphene,[88] and N-doped carbon materials[80,89,90] are most widely used to create composites with silicon. Recent research has shown that carbon deposition on the silicon's surface dampens the change of volume of silicon during cycling.[81] The initial capacity of the composite anode with graphite (50 wt% Si coated with carbon and 50 wt% graphite) is 660 mA h g^{-1} at the current density of 0.5 A g^{-1}, and the capacity drop during 450 cycles is less than 10%. Another report[86] showed that silicon embedded in CNTs results in an initial capacity of 1860 mA h g^{-1} at the current density of 0.1 A g^{-1} with 92% capacity retention after 500 cycles. Additionally, it was demonstrated[85] that a carbon coated silicon@graphene@CNT composite anode showed a capacity of 1946 mA h g^{-1} with 31% capacity loss after 100 cycles at the current density of 0.1 A g^{-1}.

Coating silicon anodes with 2 nm layer of aluminum oxynitride by atomic layer deposition increases anode capacity to 1297 mA h g^{-1}, which after 140 cycles shows the decrease by no more than 28% as a result of decreasing the side reactions at the electrode/electrolyte interface.[91] Silicon anodes can also be stabilized by deposition of an elastic organic layer of parylene (poly *p*-xylylene) that provides retention of more than 75% of capacity after 480 cycles at 0.25C.[92]

Table 3 Initial capacity and cyclic stability of modified Si-based anodes.

Material	Current density/ A g^{-1}	Initial capacity/ mA h g^{-1}	Capacity drop per cycle (%)	Cycle numbers	Ref.
Composite of graphite and porous Si coated with carbon	1	515	0.030	610	81
Composite of graphite, Si, CNT and carbon	0.2	1147	0.270	100	84
Composite of graphene, CNT and SiO_x	1	~900	~0.056	200	88
Porous composite of Si, carbon and reduced graphene oxide	1	1035	0.107	200	87
Porous Si encapsulated in carbon nanotube cage	1	1263	0.016	500	86
Poly-dopamine carbon-coated silicon/graphene/CNT composite	0.1	2430	0.200	100	85
AlO_xN_y coating on Si	0.1	1801	0.200	140	91
Parylene coating on Si	0.725	1426	0.052	480	92
Composite of C and SiO_x with polyacrylic acid binder	1	~200	0.060	1000	89
Composite of graphite and Si with lithium poly(acrylic acid) and sodium carboxymethyl cellulose binder	~0.05	~475	0.022	900	93
Si with urea formaldehyde resin grafted polyvinyl alcohol binder	2.1	3230	0.497	200	96
Si with sodium carboxymethylcellulose and thiourea binder	0.42	~2500	0.465	150	98
Si with poly(acrylic acid) and poly(ethylene oxide) binder	0.2C	3969	0.409	100	94
Si with polyacrylic acid with isocyanate-terminated polyurethane that consist of polyethylene glycol chains and 2-ureido-4-pyrimidinone binder	0.6	3692	0.167	150	95
Si with cross-linked binder carboxymethyl cellulose–phytic acid	4	1401	0.052	450	97

Binders based on polyacrylic acid,[93] polyacrylic acid and polyethylene oxide,[94] cross-linked polyacrylic acid with isocyanate-terminated polyurethane oligomers that consist of polyethylene glycol chains and 2-ureido-4-pyrimidinone,[95] formaldehyde resin grafted polyvinyl alcohol,[96] carboxymethyl cellulose/phytic acid,[97] carboxymethylcellulose sodium and thiourea,[98] poly(9,9-dioctylfluorene-*co*-fluorenone-*co*-methylbenzoic ester),[99] *etc*. have been considered as it was shown that binders containing organic acids could significantly reduce volume changes of silicon-based materials and improve their stability during cycling. The results of improving Si-based anode properties are shown in Table 3.

A lot of works were done in order to reduce the volumetric changes of silicon-based anodes by preparing their composites with carbon materials. Particular attention was paid to the choice of binder, mainly based on organic acids. This allows one to reduce the capacity drop at high current density.

2.3. Electrolytes and separators

The electrolyte is one of the key components of LIBs, which provides ion transport, determines capacity, power, operating temperature range, cyclability, and safety. A commercially used electrolyte that impregnates the porous polypropylene separator in LIBs is a 1 M solution of $LiPF_6$ in a mixture of organic carbonates (ethylene carbonate – dimethyl carbonate – diethyl carbonate).

In 2021, many efforts were put on improving electrolytes and separators for LIBs by searching for additives and new solvents capable of creating a protective SEI layer and stabilizing silicon anodes and NMC cathodes. Thus, both organic molecules and salts, such as lithium difluoro(oxalato)borate,[100] tris(trimethylsilyl) phosphite,[101,102] lithium bis(trimethylsilyl) phosphate,[103] 5,5,5′,5′-tetramethyl-2,2′-bi-1,3,2-dioxaborinane,[104] fluoroethylene carbonate[101,105,106] 1,1,1,5,5,5-hexamethyl-3-[(trimethylsilyl)oxy]-3-vinyltrisiloxane,[107] *cis*-1,2,3,6-tetrahydrophthalic anhydride,[108] 1-diphenylphosphoryloxy-4-methylbenzene,[109] *p*-toluenesulfonyl fluoride,[110] *N*-carboxyanhydrides,[111] cyclopentyl isocyanate,[112] and inorganic salts (Li_2CO_3,[113] Li_2S,[114] *etc*.) were used as electrolyte additives. The addition of *cis*-1,2,3,6-tetrahydrophthalic anhydride enhances the stability of NMC9.5.5 by creating a stable SEI that prevents side reactions and reduces resistance at the electrode/electrolyte interface. Capacity retention with the additive increased by more than 13% (up to 93.2%) after 120 cycles at 1C.[108] The addition of tris(trimethylsilyl) phosphite and fluoroethylene carbonate to the electrolyte improves the electrochemical characteristics of the Si/NMC532 cell and reduces the capacity drop during cycling by 25% in comparison with the electrolyte containing only fluoroethylene carbonate additive.[101] Moreover, the addition of lithium sulfide (0.01 mg ml^{-1}) to the electrolyte creates a stable cathode/electrolyte interface on the NMC532 surface, while the acetonitrile (0.5 vol%) suppresses the decomposition of organic carbonates due to the preferential solvation of lithium ions. Thus, the capacity drop of the graphite/NMC532 cell with the modified electrolyte decreases from 35 to 19% after 180 cycles.[112]

Modifying the standard polypropylene separator opens an opportunity to improve the electrochemical characteristics of the batteries. Thus, the possibility of increasing the capacity of the graphite/LFP cell was shown by deposition of a CoS_2/Co_3S_4 layer on the separator with subsequent lithiation, which resulted in the capacity increase from 112.6 to 150.3 mA h g^{-1} of the battery cell with the modified separator which leads to a 29.5% increase in energy density.[115]

3. Lithium metal batteries

Lithium metal batteries, where lithium metal is used as the anode, are the most promising technology for achieving high energy density <500 W h kg^{-1} and reducing battery costs, resulting in active investment in startups to develop LMBs by automotive companies. The high energy density of LMBs can be achieved as a result of the high theoretical specific capacity of lithium (~3860 mA h g^{-1}), as well as the lowest value of electrochemical potential (–3.04 V *vs*. standard hydrogen electrode).[116,117] The number of papers published on the topic of lithium metal batteries has dramatically increased recently. The main challenges limiting the commercial application of LMBs include uncontrolled Li dendrites growth during its deposition, unstable electrode/electrolyte interface, and low Coulomb efficiency caused by the formation of the SEI layer. Uncontrolled growth of lithium dendrites is caused by inhomogeneity of the SEI layer formed on the lithium anode during deposition and nonuniform deposition of lithium. Dendrites can grow and penetrate the separator film or electrolyte layer, resulting in the short circuit of the battery. A significant amount of research has focused on solving the dendrite formation in LMBs, eventually making them safer and increasing cyclability. Strategies to solve the problem include coating the surface of the lithium anode, obtaining lithium-based

composites and alloys, developing new solvents and additives for the electrolyte, or modifying the separator.

3.1. Modification of Li metal anode

3.1.1. Lithium metal coating

The formation of the SEI layer is undoubtedly a negative factor that reduces the efficiency of the batteries, especially during the first charge/discharge cycles. However, at the same time, it plays a significant role in the stabilization of the lithium/electrolyte interface to prevent dendrite formation in lithium batteries. SEI formation usually procceds through electrochemical reduction of the electrolyte, where lithium dendrite formation occurs. The composition and structure of the SEI film formed during cycling are difficult to control, thus making this SEI ineffective in suppressing dendrite formation. This resulted in many research groups developing new coatings on Li metal (sometimes called 'artificial SEI') with high mechanical strength and lithium conductivity; in addition, those coatings must be stable with different electrolytes and suppress electrolyte reduction. Thus, one can conclude that it is crucial to pay attention to the protection of the anode during cycling.

The inorganic coatings that can be employed include lithium-conducting materials with low electronic conductivity, such as Li_2Se,[118] $LiNbO_3$,[119] Li_3Bi–LiBr,[120] Li_2O,[121,122] $LiCoO_2$,[123] Li_3N,[124,125] Li_3Sb,[126] LiF,[125–128] Li_3Mg_7,[128] *etc*. Recently, it was shown that the formation of a Li_2Se layer on a lithium anode increases cycling stability at high current densities (<600 cycles at a current density of 10 mA cm^{-2}) and prevents dendrite growth.[118] The application of a Li_3Bi–LiBr protective layer on the lithium metal can increase the lifetime of the Li/$LiNbO_3$@$LiCoO_2$ cell with the $Li_7P_3S_{11}$ ceramic electrolyte up to 2000 h at the current density of less than 0.5 mA h g^{-1}, as well as increase the battery capacity by 19%.[120] The $LiCoO_2$ and carbon layers provide stable battery cycling for 1960 h at the current density of 2 mA cm^{-2} with low overpotential (~20 mV).[123] The coating layer of Li_3Sb and LiF on the lithium metal surface results in uniform deposition of lithium and symmetrical cells stability during cycling for over 400 h at the current density of 3 mA cm^{-2}.[126] Additionally, Li/LFP cell with a LiF/Li_3Mg_7 protective layer shows 134.5 mA h g^{-1} capacity at 1C rate with subsequent 1.4% capacity drop after 200 cycles.[128] Treatment of the lithium foil with 2-(fluorosulfonyl)difluoroacetic acid creates a coating layer enriched with lithium fluoride and sulfide which successfully suppresses dendrite growth. Symmetrical cells with ethylene carbonate, dimethyl carbonate and $LiPF_6$ electrolyte show low overpotential (10 mV) and cyclic stability for 350 h.[129] Addition of nanometric copper layer and Nafion cation exchange membrane ensures stable cycling of the Li/$LiCoO_2$ cell with 90% capacity retention after 500 cycles.[130]

The use of coating layers based on organic materials for the lithium anode has attracted the attention of many research groups[131–136] due to their high strength, good adhesion to the Li anode, and improving cyclic stability. Thus, the introduction of the fluoroethylene carbonate coatings (on the anode side) and succinonitrile (on the cathode side) to the ceramic electrolyte $Li_{1.5}Al_{0.5}Ge_{1.5}(PO_4)_3$ provides a stable interface with lithium metal and high voltage Ni-rich cathodes. The cell with NMC811 cathode shows a discharge capacity of 178 mA h g^{-1} with 85.7% capacity retention after 100 cycles at 0.5C.[131] Recently, it was shown[132] that poly(vinylidene fluoride-*co*-hexafluoropropylene) (PVDF-HFP) coating doped with Al_2O_3 and $LiNO_3$ ensured stable operation of the metal anode for 1000 h at the high current density (10 mA cm^{-2}). Additionally, composite coating of halloysite nanotubes and networked polymers on the metal anode was shown to reduce dendrite growth, subsequently allowing the battery to cycle for more than 1000 h at the current density of 1 mA cm^{-2}.[133]

3.1.2. Composite anodes

The development of a 3D framework host can be considered as one way to prevent the growth of lithium dendrites, which reduces current density inhomogeneity and limits volume change by providing space for lithium pre-deposition.[137–139] Thus, Li/LFP cell with a hollow N,P-doped carbon fiber as host material provides a discharge capacity of 164 mA h g^{-1}, which decreases by 28% after 100 cycles at 0.2C.[138] Recently, it was reported that composite anodes based on modified carbon nanofibers demonstrated stable operation in a symmetric cell with liquid electrolyte for over 700 h at the current density of 5 mA h cm^{-2} with at least 94% of Coulomb efficiency.[139]

Additionally, composite anodes based on inorganic materials can be made and employed in the cell, *e.g.*, it was shown that introduction of such composite anode based on lithium, ZnO, and Ni nanosheets to the Li/LFP cell showed 80% capacity retention after 450 cycles at 1C.[140] Additionally, a symmetrical cell with $LiCu_x$ nanofibrous particles-based anode allowed to

Table 4 Parameters of stripping/platting experiments for different Li/Li cells with modified Li anode.

Anode material	Electrolyte	Current density/ mA cm^{-2}	Time/h	Ref.
Li_3Bi/LiBr layer on Li	$Li_7P_3S_{11}$	0.5	>2000	120
Li_3Sb/LiF layer on Li	1 M LiTFSI in DOL/DME (1 : 1 vol%)	3.0	>400	126
LiF/sulfide layer on Li	1 M LiTFSI in DOL/DME (1 : 1 vol%)	1.0	>1000	129
Lithiated halloysite nanotubes layer on Li	1 M LiTFSI in DOL/DME (1 : 1 vol%) with 1.0 wt% $LiNO_3$	1.0	>1000	133
Li_2Se layer on Li	1 M LiTFSI in DOL/DME (1 : 1 vol%) with 1.0 wt% $LiNO_3$	1.0	>1000	118
Li_3N layer on Li–Sb alloy	1 M $LiPF_6$ in EC/DMC/FEC (1 : 1 : 0.2 vol%)	10.0	>1100	124
$LiCoO_2$ with carbon cloth layer on Li	1 M LiTFSI in DOL/DME (1 : 1 vol%) with 1.0 wt% $LiNO_3$	2.0	>1900	123
LiF/Li_3Mg_7 layer on Li	1 M LiTFSI in DOL/DME (1 : 1 vol%)	1.0	>1800	128
$Li_{3x}La_{2/3-x}TiO_3$/polyvinylidene fluoride layer on Li	1 M $LiPF_6$ in EC/DEC (1 : 1 vol%)	3.0	>1200	127
PVDF-HFP + Al_2O_3 + $LiNO_3$ film on Li	1 M $LiPF_6$ in EC/DEC (1 : 1 vol%)	10.0	>1000	132
Planar polycyclic aromatic hydrocarbons layer on Li	1 M LiTFSI in DOL/DME (1 : 1 vol%) with 1.0 wt% $LiNO_3$	4.0	>1000	135
Nanocopper and Nafion-Li layer on Li	1 M LiTFSI in DOL/DME (1 : 1 vol%) with 1.0 wt% $LiNO_3$	1.0	>800	130
Li−Sr/SrO-doped Li_2O layer on Li	$Li_{6.4}La_3Zr_{1.4}Ta_{0.6}O_{12}$	0.5	>1000	122
Composite of carbon nanoribbons and Li	1 M $LiPF_6$ in EC/DMC/EMC (1 : 1 : 1 vol%) with 1.0% vinylene carbonate	1.0	>700	139
3D-carbon-based porous anode with a pore-size gradient	1 M $LiPF_6$ in EC/PC (1 : 1 vol%) + 10 wt% FEC	1.0	>660	137
$LiCu_x$ alloy	$Li_{6.4}La_3Zr_{1.4}Ta_{0.6}O_{12}$	0.1	>10 000	141

operate for 10000 h at a current density of 0.1 mA cm^{-2}, and a cell with $LiNi_{0.88}Co_{0.1}Al_{0.02}O_2$ cathode shows 73.4% capacity retention after 500 cycles at 0.5C rate.[141] Moreover, a Ga–In alloy nanoparticles-based anode battery demonstrates an average of 99% Coulomb efficiency for more than 400 cycles.[142]

Additionally, modification of the current collector creates a uniform flow of Li^+ ions and suppresses the dendrite growth.[143,144] Therefore, the use of nickel sulfide and porous nickel-based current collector provides long-term cycling of Li/LFP cell with 95.7% capacity retention after 700 cycles at 5C.[144] Approaches to improve Li metal anode stability by its modification against dendrite formation are shown in Table 4.

3.2. Electrolytes

The electrolytes used in LMBs can be divided into two large groups: solid inorganic (sulfides, oxides) and polymeric, including composite polymeric electrolytes containing inorganic particles.[145] In 2021, many research works were reported with a focus on the development of electrolyte additives, polymer electrolytes with high ionic conductivity, and the increase of electrochemical stability window and compatibility with the lithium electrode. Recent reports in this area predominantly focused on hybrid polymer electrolytes containing lithium-conducting inorganic additives. The stable electrolytes characterized by high ionic conductivity at room temperature (>1 mS cm^{-1}) have been obtained. There is also a tendency to search for new additives to widen the electrochemical stability window to enable the operation of batteries with high-voltage cathodes and formation of the protective SEI film.

3.2.1. Polymer electrolytes

Polymer electrolytes usually consist of a lithium salt and a polymer, containing a sufficiently large number of electronegative atoms to ensure solubility of the salt and its dissociation.[145] Flexible polymer electrolytes form stable contacts with electrodes during charge and discharge and have good mechanical stability. However, on the other hand, they are often characterized by insufficient ionic conductivity at room temperature.

The Théato research group[146] developed an electrolyte based on polyethylene oxide block copolymerized with polystyrene side chains and LiTFSI with ionic conductivity of 1.6×10^{-2} mS cm^{-1} at room temperature, and a symmetrical cell based on it with lithium electrodes worked stably for 1000 h at the current density of 0.3 mA cm^{-2}. Moreover, using a polymeric electrolyte based on porphyrin molecules modified with polyether chains and LiTFSI provides an initial Li/LFP battery capacity of 158 mA h g^{-1} at 0.2C rate and 60 °C, which demonstrated only 2.8% capacity decrease after 120 cycles.[147] Moreover, electrolyte based on polycarbonate with fluorinated groups and LiTFSI with an electrochemical stability window of 5 V (*vs.* Li/Li^+) and ionic conductivity of 5×10^{-2} mS cm^{-1} at room temperature was developed, and Li/NMC811 cell with this electrolyte showed 218 mA h g^{-1} capacity at 0.1C with more than 70% capacity retention after 300 cycles.[148] Additionally, Feng with coauthors have developed a single-ion conducting polymer electrolyte containing 4-styrenesulfonyl[4-(trifluoromethoxy)benzenesulfonyl]imide functional groups with 2×10^{-2} mS cm^{-1} ionic conductivity at 30 °C.[149]

Evidently, the conductivity values of most solid polymer/salt and single-ion conducting polymer electrolytes are insufficient for effective battery operation at high current densities. Therefore, the strategies such as solvent intercalation,[150–153] obtaining copolymers to reduce the degree of crystallinity,[146,147,154] preparation of composite polymer electrolytes containing inorganic particles,[155–164] or applying several approaches simultaneously can be applied.

The electrolytes obtained by solvation with organic aprotic solvents are called gel-polymer electrolytes. Those electrolytes represent a spatial grid formed by macromolecules or their aggregates where a salt solution is distributed in a polar aprotic solvent, and as the result of solvent intercalation, an increase in the degree of salt dissociation and enhancement of polymer plasticity can be achieved.[145] Thus, the following process is often referred to as plasticization. Additionally, this process leads to an increase of the polymer segments mobility caused by solvation and increased plasticity since the ionic mobility in these materials correlates with the reorientation of coordination polyhedrons formed, among others, by electronegative polymer atoms.

The gel-polymer electrolyte based on PVDF, reinforced with polypropylene, and plasticized with $LiClO_4$ solution in dimethylformamide, demonstrated an ionic conductivity of 0.153 mS cm^{-1} at room temperature. The specific capacity of the battery with LFP cathode was shown to be 134 mA h g^{-1} with 97% capacity retention after 180 cycles at 0.3C.[150] Recently, it was demonstrated that polymer electrolytes based on a PVDF matrix plasticized with a solution of lithium difluoro(oxalato)-borate, lithium bis(fluorosulfonyl)imide (LiFSI), and $LiPF_6$ in nonflammable fluorinated carbonates (fluoroethylene carbonate, methyl 2,2,2-trifluoroethyl carbonate, ethylene carbonate) showed a high ionic conductivity of 4.41 mS cm^{-1} at 30 °C and a wide electrochemical stability window of 5.6 V (*vs.* Li/Li^+).[152] Additionally, Li/LFP batteries with this electrolyte showed a reduction of dendrite growth and 81.2% capacity retention after 1000 cycles at 1C.[152]

Another approach to improve the ionic conductivity of solid polymer electrolytes is to create their composites with lithium-conducting inorganic materials, such as $Li_7La_3Zr_2O_{12}$ (LLZO),[155–157] $Li_{6.4}La_3Zr_{1.4}Ta_{0.6}O_{12}$ (LLZTO),[158–160] $Li_{1/3}La_{5/9}TiO_3$ (LLTO),[161] $Li_{1.5}Al_{0.5}Ge_{1.5}(PO_4)_3$ (LAGP),[162,163] $Li_{1.3}Al_{0.3}Ti_{1.7}(PO_4)_3$ (LATP),[161–164] $Li(Sr,Zr)_2(PO_4)_3$,[165] $LiTa_2PO_8$,[166] *etc.* (Table 5). It has been shown that the introduction of lithium-conducting inorganic particles into cation-exchange membranes can increase lithium transfer numbers and improve cyclability of LMBs.[164,167] The polymer matrix in these materials improves the interfacial contact between the solid electrolyte and the electrodes, while the lithium-conducting inorganic additive increases the concentration of Li^+ cations, thus improving ionic conductivity. In addition, the introduction of ceramic fillers can improve the mechanical properties of the polymer matrix and inhibit the growth of lithium dendrites, *e.g.*, a three-layer membrane electrolyte based on PVDF-HFP, LiTFSI, aluminum-doped $Li_7La_3Zr_2O_{12}$ and succinonitrile showed high ionic conductivity values (0.47 mS cm^{-1}) and stable cycling performance; additionally, when the NMC622 cathode was used, 85% capacity retention was observed after 627 cycles at 0.5C.[155] The use of an electrolyte based on polyethylene oxide, aramid nanofibers, LiTFSI and $Li_7La_3Zr_2O_{12}$ with an ionic conductivity of 1.36 mS cm^{-1} at 30 °C provides an initial capacity of the Li/LFP cell of 152 mA h g^{-1} with no more than 12% capacity loss after 400 cycles.[156]

The introduction of inert inorganic particles into the gel-polymer electrolytes containing lithium salts can improve the battery's performance, which can be explained by the compositional effect promoted by the sorption processes occurring on the surface of nanoparticles.[168] Thus, SiO_2 introduction into the polyacrylonitrile matrix by hydrolysis of tetraethoxysilane followed by solvation with LiTFSI solution in 1-ethyl-3-methylimidazolium bis(trifluoromethylsulfonyl)imide (EMIMTFSI) ionic liquid provides an ionic conductivity of 0.35 mS cm^{-1}. The Li/NMC622 cell with this electrolyte showed 173 mA h g^{-1} discharge capacity and 93.7% capacity retention

Table 5 Parameters of stripping/platting experiments for different Li/Li cells with hybrid polymer/inorganic electrolytes.

Inorganic part	Polymer part	Conductivity/ mS cm^{-1}	Current density/ mA cm^{-2}	Time/h	Ref.
$Li_{6.25}Al_{0.25}La_3Zr_2O_{12}$ (12 wt%)	PVDF-HFP + LiTFSI + succinonitrile	0.48 (25 °C)	0.1–1.0	>800	155
$Li_7La_3Zr_2O_{12}$ (20 wt%)	Polyethylene oxide, aramid nanofibers + LiTFSI	1.36 (30 °C)	0.2	>400	156
$Li_{6.4}La_3Zr_{1.4}Ta_{0.6}O_{12}$ (20 wt%)	Polyacrylonitrile, polyethylene oxide + LiTFSI	0.6 (60 °C)	0.1	>500 (at 60 °C)	158
$LiTa_2PO_8$ (15 wt%)	Polyethylene oxide + LiTFSI	0.46 (60 °C)	0.1	>500 (at 60 °C)	166
$Li_{1.5}Al_{0.5}Ge_{1.5}(PO_4)_3$ (33.8 wt%)	Poly(ethylene glycol) methyl ether methacrylate + LiTFSI	0.15	0.5	>400 (at 60 °C)	162
$Li_{6.4}La_3Zr_{1.4}Ta_{0.6}O_{12}$ (3 wt%)	Poly(vinylene carbonate) + lithium difluoro(oxalato) borate	0.08 (30 °C)	0.05	>800 (at 60 °C)	159
$Li_{1.3}Al_{0.3}Ti_{1.7}(PO_4)_3$ (10 wt%) + + $Li_{0.33}La_{0.557}TiO_3$ (10 wt%)	PVDF + $LiClO_4$	~0.16 (25 °C)	1.0	>1000	161
$Li_{6.4}La_3Zr_{1.4}Ta_{0.6}O_{12}$ (10 wt%)	PVDF + HFP, polyethylene oxide + LiTFSI	0.62 (80 °C)	0.1	>3000 (at 60 °C)	160
$Li_{6.28}La_3Zr_2Al_{0.24}O_{12}$ (20 wt%)	PVDF/poly(ethylene carbonate) + LiTFSI + succinonitrile	0.39 (room temperature)	0.1	>450	157
$Li_{1.3}Al_{0.3}Ti_{1.7}(PO_4)_3$	Lithium 4-styrenesulfonyl (trifluoromethanesulfonyl) imide, poly[bis(2-(2-methoxyethoxy)ethoxy)-phosphazene] + EC/DMC (1 : 1 vol%)	0.31 (25 °C)	0.1	>2000	164
$Li_7La_3Zr_2O_{12}$ (64 wt%)	Fluoroboron-centered Li-conductive polymer framework + EC/PC	0.13 (40 °C)	0.5	>250	167

after 200 cycles, while for the cell with unmodified polyacrylonitrile 31.7% capacity retention after 100 cycles was observed.[169] Additionally, it was demonstrated that the Li/LFP battery with an electrolyte based on polyethylene oxide, LiTFSI, and MgF_2 nanofibers (0.14 mS cm^{-1} ionic conductivity at 30 °C) showed 140.6 mA h g^{-1} capacity with only 27% decrease after 500 cycles at 50 °C.[170]

3.2.2. Additives for liquid electrolyte

The reduction of standard carbonate electrolytes during battery operation creates a SEI that cannot prevent lithium dendrite sprouting. Introducing electrolyte additives of different nature can improve the SEI structure, *e.g.*, the addition of $RbNO_3$ to the electrolyte can improve the stability of Li/NMC811 batteries, ensuring 93.7% capacity retention after 200 cycles at 1C.[171] Additionally, the introduction of fluorinated solvents, such as fluoroethylene carbonate, difluoroethylene carbonate, and fluorosulfonate, can significantly increase the stability of lithium metal during battery operation, which can be explained by increased LiF content in SEI.[172–174] Moreover, the addition of 5 wt% lithium cyano tris(2,2,2-trifluoroethyl) borate provides significant improvement of electrochemical characteristics of Li/NMC532 cells as a result of the formation of a thin SEI layer containing LiF with boron and nitrogen inclusion.[175] Additions of lithium nitrate and lithium difluoro(bisoxalato) phosphate to the electrolyte lead to the formation of SEI films containing LiF and Li_3N on the lithium metal anode, as well as on an NMC811 cathode, thus leading to an increase of the Li/NMC622 cell lifetime up to 600 cycles at 0.5C with 81% capacity retention.[176] Addition of *N*,*O*-bis(trimethylsilyl) trifluoro acetamide to the electrolyte promotes the formation of LiF containing SEI with silicone and nitrogen inclusion on the metal anode's surface and on NMC811 cathode, thus leading to increased stability of the battery.[177]

4. Conclusions

This review covers the main progress in developing new materials for lithium-ion and lithium metal batteries based on data from research works published in 2021. In the field of cathode materials for lithium-ion batteries, most of the reports were focused on the increase of the cyclic stability of cathodes based on nickel-rich layered lithium–nickel–cobalt–manganese oxides (Ni-rich NMC), which can be achieved by their doping with cations capable of holding both Li^+ and transition metal positions, and by applying protective coating layers on the oxide surface (organic polymers and inorganic materials). Among anode materials, silicon-based anodes, which have a high theoretical capacity, attracted the interest of many research groups. The main disadvantage of such anodes is degradation due to a sharp volumetric change during battery operation. The following effective strategies to dampen the associated strain can be outlined: the use of porous silicon structures; formation of composites with carbon materials; coating of silicon-based particles with inorganic or polymeric materials, and substitution of standard binder materials with materials based on organic acids. Lithium metal batteries are seen as one of the most promising replacement for lithium-ion batteries. To address lithium dendrite formation in such systems, the following approaches have been proposed: the formation of stable coating layers on the lithium metal surface, obtaining composite anodes and alloys, and changing the composition of electrolytes. At the same time, in the field of electrolyte development, many efforts were put into the search for new hybrid polymer electrolytes containing lithium-conducting inorganic particles.

This work was financially supported by the Russian Science Foundation project no. 21-73-10149, https://rscf.ru/project/21-73-10149.

References

1 J. Tian, L. Yu, R. Xue, S. Zhuang and Y. Shan, *Appl. Energy*, 2022, **307**, 118205.
2 A. Y. Alent'ev, A. V. Volkov, I. V. Vorotyntsev, A. L. Maksimov and A. B. Yaroslavtsev, *Membr. Membr. Technol.*, 2021, **3**, 255.
3 A. B. Yaroslavtsev, I. A. Stenina and D. V. Golubenko, *Pure Appl. Chem.*, 2020, **92**, 1147.
4 S. Koohi-Fayegh and M. A. Rosen, *J. Energy Storage*, 2020, **27**, 101047.
5 S. P. Filippov and A. B. Yaroslavtsev, *Russ. Chem. Rev.*, 2021, **90**, 627.
6 M. M. Petrov, A. D. Modestov, D. V. Konev, A. E. Antipov, P. A. Loktionov, R. D. Pichugov, N. V. Kartashova, A. T. Glazkov, L. Z. Abunaeva, V. N. Andreev and M. A. Vorotyntsev, *Russ. Chem Rev.*, 2021, **90**, 677.
7 A. B. Yaroslavtsev and I. A. Stenina, *Mendeleev Commun.*, 2021, **31**, 423.
8 A. Masias, J. Marcicki and W. A. Paxton, *ACS Energy Lett.*, 2021, **6**, 621.
9 https://uscar.org/usabc/ 26.01.2022.
10 J. Dunn, M. Slattery, A. Kendall, H. Ambrose and S. Shen, *Environ. Sci. Technol.*, 2021, **55**, 5189.
11 J. Hu, Q. Wang, B. Wu, S. Tan, Z. Shadike, Y. Bi, M. S. Whittingham, J. Xiao, X.-Q. Yang and E. Hu, *ACS Appl. Mater. Interfaces*, 2021, **13**, 2622.

12 J. Baars, T. Domenech, R. Bleischwitz, H. E. Melin and O. Heidrich, *Nat. Sustain.*, 2021, **4**, 71.
13 C. Xu, P. J. Reeves, Q. Jacquet and C. P. Grey, *Adv. Energy Mater.*, 2021, **11**, 2003404.
14 C. S. Yoon, K.-J. Park, U.-H. Kim, K. H. Kang, H.-H. Ryu and Y.-K. Sun, *Chem. Mater.*, 2017, **29**, 10436.
15 S. Yang, Y. Zhang, Z. Li, N. Takenaka, Y. Liu, H. Zou, W. Chen, M. Du, X.-J. Hong, R. Shang, E. Nakamura, Y.-P. Cai, Y.-Q. Lan, Q. Zheng, Y. Yamada and A. Yamada, *ACS Energy Lett.*, 2021, **6**, 1811.
16 Q. Tao, L. Wang, C. Shi, J. Li, G. Chen, Z. Xue, J. Wang, S. Wang and H. Jin, *Mater. Chem. Front.*, 2021, **5**, 2607.
17 J. Zheng, P. Yan, J. Zhang, M. H. Engelhard, Z. Zhu, B. J. Polzin, S. Trask, J. Xiao, C. Wang and J. Zhang, *Nano Res.*, 2017, **10**, 4221.
18 L. Mu, R. Lin, R. Xu, L. Han, S. Xia, D. Sokaras, J. D. Steiner, T.-C. Weng, D. Nordlund, M. M. Doeff, Y. Liu, K. Zhao, H. L. Xin and F. Lin, *Nano Lett.*, 2018, **18**, 3241.
19 R. Dang, Y. Qu, Z. Ma, L. Yu, L. Duan and W. Lu, *J. Phys. Chem. C*, 2021, **121**, 151.
20 W. Xiao, Y. Nie, C. Miao, J. Wang, Y. Tan and M. Wen, *J. Colloid Interface Sci.*, 2022, **607**, 1071.
21 T. L. Kulova, I. M. Gavrilin, Yu. O. Kudryashova and A. M. Skundin, *Mendeleev Commun.*, 2020, **30**, 775.
22 A. Sannyal, K. Byun, S. A. Mian and J. Jang, *J. Phys. Chem. C*, 2021, **125**, 27543.
23 Y. Shen, X. Yao, S. Wang, D. Zhang, D. Yin, L. Wang and Y. Cheng, *ACS Appl. Mater. Interfaces*, 2021, **13**, 58871.
24 Z. Feng, S. Zhang, R. Rajagopalan, X. Huang, Y. Ren, D. Sun, H. Wang and Y. Tang, *ACS Appl. Mater. Interfaces*, 2021, **13**, 43039.
25 Y. Xi, M. Wang, L. Xu, H. M. K. Sari, W. Li, J. Hu, Y. Cao, L. Chen, L. Wang, X. Pu, J. Wang, Y. Bai, X. Liu and X. Li, *ACS Appl. Mater. Interfaces*, 2021, **13**, 57341.
26 Z. Cui, Q. Xie and A. Manthiram, *ACS Appl. Mater. Interfaces*, 2021, **13**, 15324.
27 Y. Cheng, Z. Wu, X. Dai, J. Hu, Z. Tai, J. Sun, Y. Liu, Q. Tan and Y. Liu, *J. Colloid Interface Sci.*, 2022, **605**, 718.
28 X. Ji, X. Dai, F. Wu, Y. Mai, H. Chen and Y. Gu, *Ceram. Int.*, 2021, **47**, 32043.
29 T. B. Magdaline and A. V. Murugan, *ACS Appl. Energy Mater.*, 2021, **4**, 11419.
30 X. Zhang, P. Zhang, T. Zeng, Z. Yu, X. Qu, X. Peng, Y. Zhou, X. Duan, A. Dou, M. Su and Y. Liu, *ACS Appl. Energy Mater.*, 2021, **4**, 8641.
31 X. Qu, H. Huang, T. Wan, L. Hu, Z. Yu, Y. Liu, A. Dou, Y. Zhou, M. Su, X. Peng, H.-H. Wu, T. Wu and D. Chu, *Nano Energy*, 2022, **91**, 106665.
32 S. K. Mylavarapu, F. Ulu Okudur, S. Yari, D. De Sloovere, J. D'Haen, A. Shafique, M. K. Van Bael, M. Safari and A. Hardy, *ACS Appl. Energy Mater*., 2021, **4**, 10493.
33 Y. Liu, W. Liu, M. Zhu, Y. Li, W. Li, F. Zheng, L. Shen, M. Dang and J. Zhang, *J. Alloys Compd.*, 2021, **888**, 161594.
34 Q. Fan, K. Lin, Z. Shi, S. Guan, J. Chen, S. Feng and L. Liu, *ACS Appl. Energy Mater.*, 2021, **4**, 10012.
35 X. Xie, H. Li, S. Cao, C. Wu, Z. Li, B. Chang, G. Chen, X. Guo, T. Wu and X. Wang, *Energy Fuels*, 2021, **35**, 14148.
36 Y. Zhang, C. Cui, J. Liu, Y. Bei, Y. Li, Z. Song, Y. Feng, H. Xu, S. Tian, Y. Song and F. Li, *J. Alloys Compd.*, 2021, **887**, 161480.
37 S. H. Akella, S. Taragin, Y. Wang, H. Aviv, A. C. Kozen, M. Zysler, L. Wang, D. Sharon, S. B. Lee and M. Noked, *ACS Appl. Mater. Interfaces*, 2021, **13**, 61733.
38 Z. Zhao, Y. Liu, B. Luo, J. Shen, C. Wang, J. Zhang, L. Cheng, Z. Xiao, L. Ming, B. Zhang and X. Ou, *Appl. Surf. Sci.*, 2021, **570**, 151017.
39 L. Peng, H. Ren, J. Zhang, S. Chen, C. Yu, X. Miao, Z. Zhang, Z. He, M. Yu, L. Zhang, S. Cheng and J. Xie, *Energy Storage Mater.*, 2021, **43**, 53.
40 X. Fan, X. Ou, W. Zhao, Y. Liu, B. Zhang, J. Zhang, L. Zou, L. Seidl, Y. Li, G. Hu, C. Battaglia and Y. Yang, *Nat. Commun.*, 2021, **12**, 5320.
41 Y. Li, L. Cui, C. Tan, X. Fan, Q. Pan, Y. Chu, S. Hu, F. Zheng, H. Wang and Q. Li, *Chem. Eng. J.*, 2022, **430**, 132985.
42 B. Shen, X. Xu, W. Liu, M. Qin and W. Wang, *ACS Appl. Energy Mater.*, 2021, **4**, 12917.
43 W. Shu, Z. Jian, J. Zhou, Y. Zheng and W. Chen, *ACS Appl. Mater. Interfaces*, 2021, **13**, 54916.
44 S. Hu, J. Wang, Y. Lu, L. Yang, L. Xiong, S. Zhao, L. Bai, C. Huang, C. Zhou, J. Zhu, W.-Y. Zhou, Y. Zhou and Y. Yang, *Appl. Surf. Sci.*, 2022, **579**, 152183.
45 S.-Y. Yang, Z. Shadike, W.-W. Wang, X.-Y. Yue, H.-Y. Xia, S.-M. Bak, Y.-H. Du, H. Li and Z.-W. Fu, *Energy Storage Mater.*, 2022, **45**, 1165.
46 A. B. Yaroslavtsev, *Russ. Chem. Rev.*, 2016, **85**, 1255.
47 T. Sattar, S.-H. Lee, S.-J. Sim, B.-S. Jin and H.-S. Kim, *Electrochim. Acta*, 2021, **399**, 139417.
48 Z. Zhu, J. Duan, J. Zhang, S. Zhou, X. Huang, Q. Meng, P. Dong and Y. Zhang, *Chem. Eng. J.*, 2022, **430**, 132908.
49 I. A. Stenina and A. B. Yaroslavtsev, *Pure Appl. Chem.*, 2017, **89**, 1185.
50 K. Lin, S. Yang, Z. Shi, Q. Fan, Z. Liu and L. Liu, *J. Power Sources*, 2022, **520**, 230768.
51 https://www.argusmedia.com/en/news/2282543-chinas-november-power-battery-output-hits-new-high 26.01.2022.
52 Q. Zhao, S. Zhang, M. Hu, C. Wang and G. Jiang, *Int. J. Electrochem. Sci.*, 2021, **16**, 211226.
53 Y.-M. Xin, H.-Y. Xu, J.-H. Ruan, D.-C. Li, A.-G. Wang and D.-S. Sun, *Int. J. Electrochem. Sci.*, 2021, **16**, 210655.
54 S. A. Yaroslavtsev, N. I. Vostrov, S. A. Novikova, T. L. Kulova, A. B. Yaroslavtsev and V. S. Rusakov, *J. Phys. Chem. C*, 2020, **124**, 13026.
55 A. B. Yaroslavtsev, T. L. Kulova and A. M. Skundin, *Russ. Chem. Rev.*, 2015, **84**, 826.
56 M. A. M. M. Alsamet and E. Burgaz, *Electrochim. Acta*, 2021, **367**, 137530.
57 S. A. Novikova and A. B. Yaroslavtsev, *Rev. Adv. Mater. Sci.*, 2017, **49**, 129.
58 Y. Li, L. Wang, K. Zhang, F. Liang, Y. Yao and L. Kong, *J. Alloys Compd.*, 2022, **890**, 161617.
59 W. Li, A. Garg, M. L. P. Le, C. Ruhatiya, L. Gao and V. M. Tran, *Electrochim. Acta*, 2020, **330**, 135314.
60 I. A. Stenina, P. V. Minakova, T. L. Kulova, A. V. Desyatov and A. B. Yaroslavtsev, *Inorg. Mater.*, 2021, **57**, 620.
61 A. B. Yaroslavtsev and I. A. Stenina, *Surf. Innov.*, 2021, **9**, 92.
62 C. Y. Huang, T. R. Kuo, S. Yougbaré and L. Y. Lin, *J. Colloid Interface Sci.*, 2022, **607**, 1457.
63 M. Shi, R. Li and Y. Liu, *J. Alloys Compd.*, 2021, **854**, 157162.
64 X. Chen, Y. Li and J. Wang, *Nanomaterials*, 2021, **11**, 12.
65 V. V. Ozerova, I. A. Stenina, A. A. Kuz'mina, T. L. Kulova and A. B. Yaroslavtsev, *Inorg. Mater.*, 2020, **56**, 648.
66 S. Huang, H. Chen, M. Chen, Y. Huang, X. He, H. Zhuo and S. Chen, *ACS Sustainable Chem. Eng.*, 2021, **9**, 13277.
67 M. Jiang, Y. Ma, J. Chen, W. Jiang and J. Yang, *Nanoscale*, 2021, **13**, 3937.
68 I. Stenina, R. Shaydullin, T. Kulova, A. Kuz'mina, N. Tabachkova and A. Yaroslavtsev, *Energies*, 2020, **13**, 3941.
69 I. A. Stenina, R. R. Shaydullin, A. V. Desyatov, T. L. Kulova and A. B. Yaroslavtsev, *Electrochim. Acta*, 2020, **364**, 137330.
70 I. A.Stenina, A. N. Sobolev, T. L. Kulova and A. B. Yaroslavtsev, *Inorg. Mater.*, 2022, **58**, 154.
71 D. Yarmolich, Y. Odarchenko, C. Murphy, E.A. Petrucco, J. Cookson, D. Yarmolich, T. Zhao, H.-K. Kim, R. V. Kumar and R. I. Tomov, *Nano Energy*, 2021, **83**, 105816.
72 M. Trukawka, K. Wenelska, L. Singer, R. Klingeler, X. Chen and E. Mijowska, *J. Alloys Compd.*, 2021, **853**, 156700.
73 J. Kriegler, L. Hille, S. Stock, L. Kraft, J. Hagemeister, J. B. Habedank, A. Jossen and M. F. Zaeh, *Appl. Energy*, 2021, **303**, 117693.
74 Z. Wang, K. Kang, J. Wu, Q. Hu, D. P. Harper, G. Du, S. Wang and K. Xu, *J. Mater. Res. Technol.*, 2021, **11**, 50.
75 Z. Wang, B. Xing, H. Zeng, G. Huang, X. Liu, H. Guo, C. Zhang, Y. Cao and Z. Chen, *Appl. Surf. Sci.*, 2021, **547**, 149228.
76 S. N. Faisal, C. M. Subramaniyam, M. M. Islam, A. I. Chowdhury, S. X. Dou, A. K. Roy, A. T. Harris and A. I. Minett, *J. Alloys Compd.*, 2021, **850**, 156701.
77 M. Salah, C. Hall, P. Murphy, C. Francis, R. Kerr, B. Stoehr, S. Rudd and M. Fabretto, *J. Power Sources*, 2021, **506**, 230194.
78 P. Li, H. Kim, S.-T. Myung and Y.-K. Sun, *Energy Storage Mater.*, 2021, **35**, 550.
79 Z. Liu, Q. Yu, Y. Zhao, R. He, M. Xu, S. Feng, S. Li, L. Zhou and L. Mai, *Chem. Soc. Rev.*, 2019, **48**, 285.
80 X. Guo, W. Li, P. Geng, Q. Zhang, H. Pang and Q. Xu, *J. Colloid Interface Sci.*, 2022, **606**, 784.
81 N. Yoon, C. H. Young, D. Kang, H. Park and J. K. Lee, *Electrochim. Acta*, 2021, **391**, 138967.
82 G. Yang, S. Frisco, R. Tao, N. Philip, T. H. Bennett, C. Stetson, J.-G. Zhang, S.-D. Han, G. Teeter, S. P. Harvey, Y. Zhang, G. M. Veith and J. Nanda, *ACS Energy Lett.*, 2021, **6**, 1684.
83 Z. Feng, W. Peng, Z. Wang, H. Guo, X. Li, G. Yan and J. Wang, *Int. J. Miner., Metall. Mater.*, 2021, **28**, 1549.
84 Y. Huang, W. Li, J. Peng, Z. Wu, X. Li and X. Wang, *Energy Fuels*, 2021, **35**, 13491.
85 F. Wang, S. Lin, X. Lu, R. Hong and H. Liu, *Electrochim. Acta*, 2022, **404**, 139708.
86 Y. Ren, X. Yin, R. Xiao, T. Mu, H. Huo, P. Zuo, Y. Ma, X. Cheng, Y. Gao, G. Yin, Y. Li and C. Du, *Chem. Eng. J.*, 2022, **431**, 133982.

87 Q. Chang, L. Yao, W. Zha, M. Wu, F. Xu and Z. Wen, *ACS Appl. Energy Mater.*, 2021, **5**, 380.
88 J. Zhang, G. Yang, J.-A. Wang, Z.-L. Hou, X. Zhang and C. Li, *Energy Fuels*, 2021, **35**, 19784.
89 S. Kumagai, Y. Abe, M. Tomioka and M. Kabir, *Sci. Rep.*, 2021, **11**, 15784.
90 Z. Yang, M. Jiang, X. Wang, Y. Wang and M. Cao, *ACS Appl. Mater. Interfaces*, 2021, **13**, 52636.
91 H. Zhu, M. H. A. Shiraz, L. Liu, Y. Zhang and J. Liu, *Appl. Surf. Sci.*, 2022, **578**, 151982.
92 N. Harpak, G. Davidi and F. Patolsky, *Chem. Eng. J.*, 2022, **429**, 132077.
93 N. Hamzelui, G. G. Eshetu and E. Figgemeier, *J. Energy Storage*, 2021, **35**, 102098.
94 Y. Hu, D. Shao, Y. Chen, J. Peng, S. Dai, M. Huang, Z.-H. Guo, X. Luo and K. Yue, *ACS Appl. Energy Mater.*, 2021, **4**, 10886.
95 Z. Liu, C. Fang, X. He, Y. Zhao, H. Xu, J. Lei and G. Liu, *ACS Appl. Mater. Interfaces*, 2021, **13**, 46518.
96 W. Wang, Y. Li, Y. Wang, W. Huang, L. Lv, G. Zhu, Q. Qu, Y. Liang, W. Zheng and H. Zheng, *Electrochim. Acta*, 2021, **400**, 139442.
97 Z. Zheng, H. Gao, C. Ke, M. Li, Y. Cheng, D.-L. Peng, Q. Zhang and M.-S. Wang, *ACS Appl. Mater. Interfaces*, 2021, **13**, 53818.
98 T.-T. Su, W.-F. Ren, K. Wang, J.-M. Yuan, C.-Y. Shao, J.-L. Ma, X.-H. Chen, L.-P. Xiao and R.-C. Sun, *Electrochim. Acta*, 2022, **402**, 139552.
99 T. Zhu and G. Liu, *J. Electrochem. Soc.*, 2021, **168**, 050533.
100 E. Zhao, S. Luo, Y. Gu, L. Yang and S. Hirano, *ACS Appl. Mater. Interfaces*, 2021, **13**, 59843.
101 A. K. Haridas, Q. A. Nguyen, T. Terlier, R. Blaser and S. L. Biswal, *ACS Appl. Mater. Interfaces*, 2021, **13**, 2662.
102 J. Kim, V. A. K. Adiraju, N. Rodrigo, J. Hoffmann, M. Payne and B. L. Lucht, *ACS Appl. Mater. Interfaces*, 2021, **13**, 22351.
103 J. Kim, V. A. K. Adiraju, O. B. Chae and B. L. Lucht, *J. Electrochem. Soc.*, 2021, **168**, 080538.
104 Y. Zou, G. Liu, K. Zhou, J. Zhang, T. Jiao, X. Zhang, Y. Yang and J. Zheng, *ACS Appl. Energy Mater.*, 2021, **4**, 11051.
105 A. D. Pathak, K. Samanta, K. K. Sahu and S. Pati, *J. Appl. Electrochem.*, 2021, **51**, 143.
106 N. N. Intan and J. Pfaendtner, *ACS Appl. Mater. Interfaces*, 2021, **13**, 8169.
107 H.-S. Kim, T. H. Kim, S. S. Park, M. S. Kang and G. Jeong, *ACS Appl. Mater. Interfaces*, 2021, **13**, 44348.
108 X. Zhang, G. Liu, T. Jiao, Y. Cheng, Y. Zou, M.-C. Wang, Y. Yang and J. Zheng, *ACS Appl. Energy Mater*., 2021, **4**, 12275.
109 P. Yan, Y. Zhu, X. Pan and H. Ji, *Int. J. Energy Res*., 2021, **45**, 2776.
110 Y. Che, X. Lin, L. Xing, X. Guan, R. Guo, G. Lan, Q. Zheng, W. Zhang and W. Li, *J. Energy Chem.*, 2021, **52**, 361.
111 J.-P. Schmiegel, R. Nölle, J. Henschel, L. Quach, S. Nowak, M. Winter, F. Glorius and T. Placke, *Cell Rep. Phys. Sci.*, 2021, **2**, 100327.
112 G. Liu, N. Xu, Y. Zou, K. Zhou, X. Yang, T. Jiao, W. Yang, Y. Yang and J. Zheng, *ACS Appl. Mater. Interfaces*, 2021, **13**, 12069.
113 S. Klein, P. Harte, J. Henschel, P. Bärmann, K. Borzutzki, T. Beuse, S. van Wickeren, B. Heidrich, J. Kasnatscheew, S. Nowak, M. Winter and T. Placke, *Adv. Energy Mater.*, 2021 **11**, 2003756.
114 X. Shi, T. Zheng, J. Xiong, B. Zhu, Y.-J. Cheng and Y. Xia, *ACS Appl. Mater. Interfaces*, 2021, **13**, 57107.
115 Z. Rao, J. Wu, B. He, W. Chen, H. Wang, Q. Fu and Y. Huang, *ACS Appl. Mater. Interfaces*, 2021, **13**, 38194.
116 J. Li, Z. Kong, X. Liu, B. Zheng, Q. H. Fan, E. Garratt, T. Schuelke, K. Wang, H. Xu and H. Jin, *InfoMat.*, 2021, **3**, 1333.
117 M. Qi, L. Xie, Q. Han, L. Zhu, L. Chen and X. Cao, *J. Energy Storage*, 2021, **47**, 103641.
118 Y. Ma, L. Wei, Y. Gu, L. Zhao, Y. Jing, Q. Mu, Y. Su, X. Yuan, Y. Peng and Z. Deng, *Nano Lett*., 2021, **21**, 7354.
119 M. Jiang, Q. Zhang, D. L. Danilov, R.-A. Eichel and P. H. L. Notten, *ACS Appl. Energy Mater*., 2021, **4**, 10333.
120 B. Zhao, Y. Shi, J. Wu, C. Xing, Y. Liu, W. Ma, X. Liu, Y. Jiang and J. Zhang, *Chem. Eng. J.*, 2022, **429**, 132411.
121 P. B. Samarasingha, M.-T. Lee and M. Valvo, *Electrochim. Acta*, 2021, **397**, 139270.
122 X. He, X. Ji, B. Zhang, N. D. Rodrigo, S. Hou, K. Gaskell, T. Deng, H. Wan, S. Liu, J. Xu, B. Nan, B. L. Lucht and C. Wang, *ACS Energy Lett.*, 2022, **7**, 131.
123 A. Xu, J. Cui, Y. Liu, S. Zhang, B. Jin and M. Shao, *ACS Sustainable Chem. Eng.*, 2021, **9**, 14663.
124 S. Wang, J. Chen, H. Lu, Y. Zhang, J. Yang, Y. Nuli and J. Wang, *ACS Appl. Energy Mater.*, 2021, **4**, 13132.
125 S. Kim, T. K. Lee, S. K. Kwak and N.-S. Choi, *ACS Energy Lett.*, 2022, **7**, 67.
126 C. Cui, R. Zhang, C. Fu, R. Xiao, R. Li, Y. Ma, J. Wang, Y. Gao, G. Yin and P. Zuo, *Chem. Eng. J.*, 2021, **433** (**2**), 133570.
127 B. Li, Q. Su, J. Zhang, L. Yu, G. Du, S. Ding, M. Zhang, W. Zhao and B. Xu, *ACS Appl. Mater. Interfaces*, 2021, **13**, 56682.
128 L. Ai, Z. Chen, S. Li, T. Xu, J. Zhang, L. Shen and X. Zhang, *ACS Appl. Energy Mater.*, 2021, **4**, 14407.
129 J. Yang, J. Hou, Z. Fang, K. Kashif, C. Chen, X. Li, H. Zhou, S. Zhang, T. Feng, Z. Xu and M. Wu, *Chem. Eng. J.*, 2021, **433** (**2**), 133193.
130 K. Liao, Z. Li, S. Gu, Y. Li, L. Kong, N. Qin, H. Huang, S. Wu, J. Chen, Q. Gan, K. Zhang and Z. Lu, *ACS Appl. Mater. Interfaces*, 2021, **13**, 45416.
131 W. Zha, Y. Ruan and Z. Wen, *Chem. Eng. J.*, 2022, **429**, 132506.
132 D. Yang, J. Li, F. Yang, J. Li, L. He, H. Zhao, L. Wei, Y. Wang, X. Wang and Y. Wei, *Nano Lett.*, 2021, **21**, 7063.
133 H. Liu, R. Tao, C. Guo, W. Zhang, X. Liu, P. Guo, T. Zhang and J. Liang, *Chem. Eng. J.*, 2022, **429**, 132239.
134 T. Jin, M. Liu, K. Su, Y. Lu, G. Cheng, Y. Liu, N.-W. Li and L. Yu, *Mater. Interfaces*, 2021, **13**, 57489.
135 S. Chang, X. Jin, Q. He, T. Liu, J. Fang, Z. Shen, Z. Li, S. Zhang, M. Dahbi, J. Alami, K. Amine, A.-D. Li, H. Zhang and J. Lu, *Nano Lett*., 2022, **22**, 263.
136 S. Niu, S.-W. Zhang, D. Li, X. Wang, X. Chen, R. Shi, N. Shen, M. Jin, X. Zhang, Q. Lian, R. Huang, A. Amini, Y. Zhao and C. Cheng, *Chem. Eng. J.*, 2022, **429**, 132156.
137 H.-J. Noh, M.-H. Lee, B. G. Kim, J.-H. Park, S.-M. Lee and J.-H. Choi, *ACS Appl. Mater. Interfaces*, 2021, **13**, 55227.
138 J. Jian, Y. Zhang, J. Sun, L. Peng, C. Lu, C. Jin, H. Wang and R. Yang, *ACS Appl. Energy Mater.*, 2021, **4**, 14191.
139 J. Zhang, X. Zhao, Q. Tong, C. Li and M. Zhu, *Carbon*, 2021, **184**, 357.
140 K. Wang, W. Wang, J. Deng, X. Jiang, G. Xu, H. Gong, N. Zhang and D. Li, *J. Alloys Compd*., 2021, **889**, 161597.
141 Q. Dai, J. Zhao, H. Ye, J. Chen, Y. Su, T. Yang, Q. Liu, H. Sun, H. Li, J. Yao, Z. Gao, X. Fu, D. Zhu, J. Yan, M. Li, H. Qiu, Q. Huang, L. Zhang, Y. Tang, X. Guo and J. Huang, *ACS Appl. Mater. Interfaces*, 2021, **13**, 42822.
142 P. Zhai, L. Liu, Y. Wei, J. Zuo, Z. Yang, Q. Chen, F. Zhao, X. Zhang and Y. Gong, *Nano Lett.*, 2021, **21**, 7715.
143 W.-B. Jung, O. B. Chae, M. Kim, Y. Kim, Y. J. Hong, J. Y. Kim, S. Choi, D. Y. Kim, S. Moon, J. Suk, Y. Kang, M. Wu and H.-T. Jung, *ACS Appl. Mater. Interfaces*, 2021, **13**, 60978.
144 J. Zhang, Y. Zhou, F. Tu, Y. Ma, H. Zhang, D. Song, X. Shi and L. Zhang, *Chem. Eng. J.*, 2022, **428**, 132510.
145 D. Yu. Voropaeva, S. A. Novikova and A. B. Yaroslavtsev, *Russ. Chem. Rev*., 2020, **89**, 1132.
146 A. J. Butzelaar, P. Röring, T. P. Mach, M. Hoffmann, F. Jeschull, M. Wilhelm, M. Winter, G. Brunklaus and P. Théato, *ACS Appl. Mater. Interfaces*, 2021, **13**, 39257**.**
147 Q. Zeng, P. Chen, Z. Li, X. Wen, W. Wen, Y. Liu, H. Zhao, S. Zhang, H. Zhou and L. Zhang, *ACS Appl. Mater. Interfaces*, 2021, **13**, 48569.
148 Y. Wang, S. Chen, Z. Li, C. Peng, Y. Li and W. Feng, *Energy Storage Mater.*, 2022, **45**, 474.
149 S. Chen, Y. Li, Y. Wang, Z. Li, C. Peng, Y. Feng and W. Feng, *Macromolecules*, 2021, **54**, 9135.
150 K. Shi, Z. Xu, M. Huang, L. Zou, D. Zheng, Z. Yang and W. Zhang, *J. Membr. Sci.*, 2021, **638**, 119713.
151 B. Zhou, Y. Zhou, L. Lai, Z. Chen, J. Li, Y. Jiang, J. Liu, Z. Wang and Z. Xue, *ACS Appl. Energy Mater.*, 2021, **4**, 9582.
152 K. Deng, Z. Xu, S. Zhou, Z. Zhao, K. Zeng, M. Xiao, Y. Meng and Y. Xu, *J. Power Sources*, 2021, **510**, 230411.
153 I. A. Stenina and A. B. Yaroslavtsev, *Membranes*, 2021, **11**, 198.
154 C. Zuo, H. Li, G. Chen, J. Yang, Z. Xu and Z. Xue, *ACS Appl. Energy Mater.*, 2021, **4**, 9402.
155 S. L. Beshahwured, Y.-S. Wu, T. B. Truong, R. Jose and C.-C. Yang, *Chem. Eng. J.*, 2021, **426**, 131850.
156 J. Yin, X. Xu, S. Jiang, H. Wu, L. Wei, Y. Li, J. He, K. Xi and Y. Gao, *Chem. Eng. J.*, 2021, **431**, 133352.
157 T. H. Mengesha, S. L. Beshahwured, S.-H. Wu, Y.-S. Wu, R. Jose, S. J. Lue and C.-C. Yang, *ACS Appl. Energy Mater.*, 2021, **4**, 14554.
158 Y. Li, L. Yang, R. Dong, T. Zhang, J. Yuan, Y. Liu, Y. Liu, Y. Sun, B. Zhong, Y. Chen, Z. Wu and X. Guo, *Electrochim. Acta*, 2022, **404**, 139701.
159 X. Huang, J. Wu, X. Wang, Y. Tian, F. Zhang, M. Yang, B. Xu, B. Wu, X. Liu and H. Li, *ACS Appl. Energy Mater.*, 2021, **4**, 9368.
160 R.-A. Tong, L. Chen, B. Fan, G. Shao, R. Liu and C.-A. Wang, *ACS Appl. Energy Mater.*, 2021, **4**, 11802.

161 S. H. Siyal, S. S. A. Shah, T. Najam, M. S. Javed, M. Imran and J.-L. Lan, *ACS Appl. Energy Mater*., 2021, **4**, 8604.
162 S. Yang, Z. Zhang, L. Shen, P. Chen, Z. Gu, M. Chang, Y. Zhao, H. He and X. Yao, *J. Power Sources*, 2022, **518**, 230756.
163 E. A. Kurzina, I. A. Stenina, A. Dalvi and A. B. Yaroslavtsev, *Inorg. Mater.*, 2021, **57**, 1035.
164 S. Yu, Q. Xu, X. Lu, Z. Liu, A. Windmüller, C.-L. Tsai, A. Buchheit, H. Tempel, H. Kungl, H.-D. Wiemhöfer and R.-A. Eichel, *ACS Appl. Mater. Interfaces*, 2021, **13**, 61067.
165 H. Park, E. G. Lee, S.-Y. Kim, S. J. Seong, J. Y. Suh, M. Wu, Y. Kang, S.-Y. Choi, Y. Kim and S. Choi, *ACS Appl. Energy Mater*., 2021, **4**, 13974.
166 Y. Na, Zh. Chen, Zh. Xu, Q. An, X. Zhang, X. Sun, Sh. Cai and Ch. Zheng, *Chin. Chem. Lett.*, 2021, https://doi.org/10.1016/j.cclet.2021.12.022.
167 K. Liu, X. Li, J. Cai, Z. Yang, Z. Chen, B. Key, Z. Zhang, T. L. Dzwiniel and C. Liao, *ACS Energy Lett.*, 2021, **6**, 1315.
168 A. B. Yaroslavtsev, *Russ. J. Inorg. Chem.*, 2000, **45**, S249.
169 M. Yao, Q. Ruan, T. Yu, H. Zhang and S. Zhang, *Energy Storage Mater.*, 2022, **44**, 93.
170 W. Yu, N. Deng, Z. Yan, L. Gao, K. Cheng, X. Tian, L. Tang, B. Cheng and W. Kang, *J. Energy Chem.*, 2022, **67**, 684.
171 C. Liao, L. Han, X. Mu, Y. Zhu, N. Wu, J. Lu, Y. Zhao, X. Li, Y. Hu, Y. Kan and L. Song, *ACS Appl. Mater. Interfaces*, 2021, **13**, 46783.
172 C.-C. Su, M. He, M. Cai, J. Shi, R. Amine, N. D. Rago, J. Guo, T. Rojas, A. T. Ngo and K. Amine, *Nano Energy*, 2022, **92**, 106720.
173 D. Zhang, R. Gu, W. Guo, Q. Xu, H. Li and Y. Min, *ACS Appl. Mater. Interfaces*, 2021, **13**, 60678.
174 K. Zhang, Y. An, C. Wei, Y. Qian, Y. Zhang and J. Feng, *ACS Appl. Mater. Interfaces*, 2021, **13**, 50869.
175 O. B. Chae, V. A. K. Adiraju and B. L. Lucht, *ACS Energy Lett.*, 2021, **6**, 3851.
176 S. Kim, S. O. Park, M.-Y. Lee, J.-A. Lee, I. Kristanto, T. K. Lee, D. Hwang, J. Kim, T.-U. Wi, H.-W. Lee, S. K. Kwak and N.-S. Choi, *Energy Storage Mater*., 2022, **45**, 1.
177 Y. Liu, L. Hong, R. Jiang, Y. Wang, S. V. Patel, X. Feng and H. Xiang, *ACS Appl. Mater. Interfaces*, 2021, **13**, 57430.

Received: 25th March 2022; Com. 22/6838